JOURNAL OF MATERIALS SCIENCE 30 (1995) 2284–2290

Ion storage properties of CeO_2 and mixed CeO_2/SnO_2 coatings

Z. CRNJAK OREL, B. OREL
National Institute of Chemistry, Hajdrihova 19, 61115 Ljubljana, Slovenia

Ion storage CeO_2 and CeO_2/SnO_2 coatings were prepared by the sol–gel dip-coating method using an aqueous-based process. The influence of added SnO_2 in the CeO_2 oxide coatings on the inserted/extracted charge was determined by chronocoulometric measurements. It was found that for 60 nm thick film, the inserted/extracted charge was twice ($Q = 10$ mC cm^{-2}) as large for films containing 17 mol% SnO_2, if compared to pure CeO_2. The effect of the addition of SnO_2 to the mixed oxide coatings on their optical properties and structural characteristics was studied.

1. Introduction

The sol–gel process offers a new method of synthesizing oxide layers. In the literature [1] it is usually divided into two categories: aqueous-based processes and alcohol-based processes.

The aqueous-based process starts from a solution of metal salt, and the sol is prepared by condensation or dispersion. The dispersion method is quicker, and metal salt is hydrolysed rapidly at room temperature with an excess of base. The precipitate must be washed from the electrolyte and later peptized (dispersed) by the addition of strong acid. In the aqueous-based process, the gelation of the sol is performed by the removal of water or by an increase in the pH, if the sol is stabilized by the development of positive surface charge. It is not possible for all sols to be converted to gels. Because gels are solids containing a liquid component, and because gels are in a highly dispersed state, it is necessary that there is a strong particle solvent interaction. This means that at least part of the solvent has to be bonded.

When the sol is formed in an aqueous process, chemical homogeneity is maintained on an atomic scale for multicomponent systems, if the different metal ions co-precipitate during hydrolysis. This method (for preparation of thin films) was exploited in our work for the preparation of thin CeO_2 and CeO_2/SnO_2 films.

The fluorite-type CeO_2 lattice consists of three sublattices [2]: one Ce^{4+} ion and two non-equivalent oxygen ions (O_1^{2-} and O_2^{2-}). The space group is O_h^5 and the primitive cell contains only one formula unit. The cation-doped ceria, due to its high oxygen ionic conductivity [3], is a potential solid electrolyte for solid-oxide fuel cells. It contains vacancies in the crystal lattice because of partial replacement of host cations. Very heavy doping is possible in ceria. Most of the rare-earth oxides are very soluble, for example, the solubility for Sm_2O_3 was 50 at%. Increase of the lattice constant is in proportion to the radius of the dopant cation.

Cerium dioxide (CeO_2) has been considered as a useful material with a high-refractive index film in single- and multilayered optical coatings. Its refractive index strongly depends on a deposition parameter. CeO_2-based films are highly efficient for absorbing ultraviolet radiation, and glass with 2–4% CeO_2 is valuable in protecting light-sensitive materials [4]. The films are also used for corrosion protection of metals and as coatings for use as catalyst supports.

Sol–gel–deposited CeO_2-based films have been studied [5–7] as the counter electrode in electrochromic devices used for "smart windows". In order to improve the slow kinetics of pure CeO_2 prepared by the evaporation technique, the authors suggested that it would be suitable to substitute cerium atoms by another element of smaller radius, in order to change the structure. They chose titanium, and various Ti/Ce ratios were synthesized by the sol–gel process using $Ce(NH_4)_2(NO_3)_6$ and tetra-isopropyl orthotitanate Ti–(O-iso-$C_3H_7)_4$. It was found that cathodic and anodic peaks showed reversible insertion for lithium ions, and the charge inserted and extracted at sweep rate 10 mV was approximately 10 mC cm^{-2} for three dippings [5].

The counter electrode provides electrochemical balance of the charge transferred during the oxidation and reduction reactions performed on a primary electrochromic element [6]. It is necessary that these reactions (oxidation, reduction) be at least as reversible as those in an electrochromic element, otherwise the switching cycle lifetime will be limited.

Optically, it is possible to divide the counter electrodes into two main groups. The first one presents transparent counter electrodes, such as In_2O_3, In_2O_3/Sn, CeO_2 and V_2O_5 [5]. Unfortunately, despite the retained transparency of In_2O_3-derived layers, the insertion rate of lithium is insufficient and the reaction is partially irreversible. By contrast, CeO_2 exhibits reversibility, but the reaction kinetics is very low. V_2O_5 is reversible, and fast enough, but

0022–2461

unfortunately in the bleaching state the transmission is not adequate. The second group is characterized by an additional contribution to the optical modulation by bleaching and colouring synchronously with the primarily electrochromic layer. Some oxides were prepared as counter electrodes, for example, in the form of NiOOH [8], IrO_2 as well as mixed oxide systems. Investigation [9] into mixed oxide systems containing Li_2O, WO_3 and M_mO_n; M = Fe, Ce, Mn, V or Sb, prepared by thermal evaporation as counter electrodes revealed problems in the preparation of thin oxide films, as well as the insufficient transparency of prepared films.

Other very important requirements for counter electrodes [9], apart from high resistance to heat, and a wide operating temperature range ($-20\,^{\circ}C$, $+90\,^{\circ}C$) are that electronic conductivity should be greater than $10^{-7}\Omega^{-1}\,cm^{-1}$ at room temperature, the charge of $20\,mC\,cm^{-2}$ should be transported, lithium-ion mobility should be in the range of $10^6\,cm^2V^{-1}s^{-1}$ and, most important, it should be possible to prepare thin films [9].

In our work, the dispersion method (aqueous-based process) was used for the preparation of pure CeO_2 and mixed CeO_2/SnO_2 oxides. The sols obtained were used for the preparation of thin films on indium tin oxide (ITO) plates for counter electrodes in electrochromic devices. This method, compared to the alcohol-based method, is relatively inexpensive, because the metal sols are already available.

In the present work, the influence of added SnO_2 previously investigated [10, 11] in the mixed oxide coatings was determined by chronocoulometric measurement, UV/VIS/NIR transmittance and Fourier transform–infrared (FT–IR) spectroscopy.

2. Experimental procedure

The preparation of an aqueous dispersion of hydrated oxides (sol) of CeO_2 and mixed CeO_2/SnO_2 started from a solution of metal salt $Ce(NH_4)_3(NO_3)_6$ and $SnCl_4$ (Table I). Precipitates were obtained by addition of NH_4OH until pH = 9 was reached. After washing the precipitate in order to remove residual NH_4^+, Cl^-, NO_3^- with doubly distilled water, the peptization was performed, according to the modified method described by Atkinson [12], by addition of an equimolar quantity of HNO_3 (pH $\approx$ 1) [13]. The colloidal sols were aged for 20 min at temperatures up to 90 °C, thus yielding yellowish semitransparent sols, which turned to gel after 2 weeks at a Ce/Sn atomic ratio of 1.

The films were prepared by the dip-coating methods with a pulling speed of $10\,cm\,min^{-1}$ on ITO glass plates ($2 \times 3 \times 0.1\,cm^3$) and with repeated (eight times) dipping. To obtain good wettability, previously cleaned substrates in a chrome–sulphuric acid, were treated in a 1% solution of non-ionic surfactant (ETOLAT-138, TEOL, Ljubljana).

The EG & PAR-Mod 273 potentiostat galvanostat with electrochemical analysis software was used for cyclic voltammetric and chronocoulometric experiments. A Ramp acquisition mode was employed in all

TABLE I Schematic presentation of the aqueous sol–gel dip-coating process

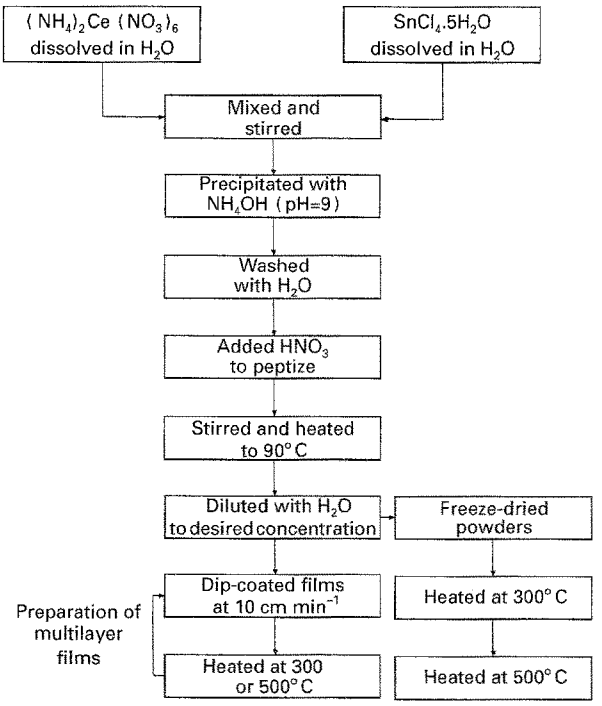

cyclic voltammetric measurements. A platinum rod and Ag/AgCl/0.2 M KCl served as counter and reference electrode, respectively. The working electrode area was $1\,cm^2$ in electrolyte solution (30 ml 0.1 M LiOH). The Metrohm-type voltammetric cell (50 ml) was used. Pure argon was bubbled through the electrolyte solution for 10 min before the measurements were started. The scanning rate was $20\,mV\,s^{-1}$. Cycling and chronocoulometric measurements were performed at potentials of + 0.4 V and − 1.3 V.

The FT–IR spectra at resolution 4 and $8\,cm^{-1}$ were recorded on Digilab FTS-80 spectrometer as transmittance (using nujol muls for preparations). Near grazing incidence angles (NGIA) at 80° of dip-coated films were recorded. Wire grid polarizers were used.

X-ray diffraction analyses of oxide powders and dip-coated films were performed on a Philips PW 1710 X-ray diffractometer. The measurements for different scanning calorimetry were performed on a DSC-910 module controlled by TA 2000 thermal analyser (TA-instrument Castle Point, DE, USA). The heating rate was $10\,^{\circ}C\,min^{-1}$ in a static air atmosphere. Transmittance spectra, in the spectral range 0.3–2.5 μm were measured by a Perkin–Elmer Lambda 9 spectrometer at a resolution of 2 nm. The T (λ) values obtained were used for the calculation of normal solar transmittance according to the equation

$$T_s = \frac{\int_{0.3\,\mu m}^{2\,\mu m} T(\lambda) P_s(\lambda) d\lambda}{\int_{0.3\,\mu m}^{2\,\mu m} P_s(\lambda)\, d\lambda} \qquad (1)$$

where $P_s(\lambda)$ is solar spectrum at an air mass of 2.

The surface Profiler Alfa Step 200 was used for thickness measurements.

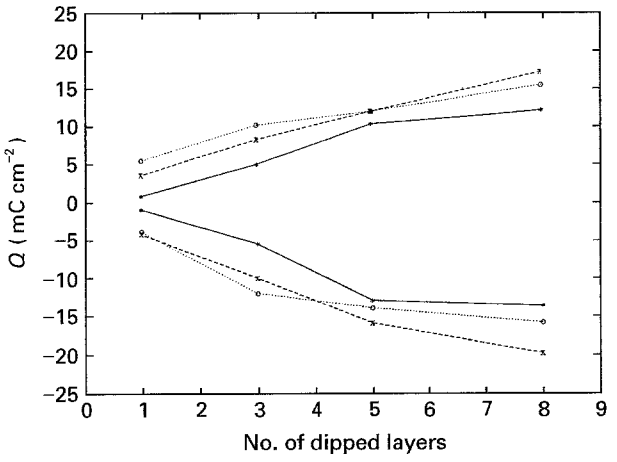

Figure 1 Cathodic and anodic total charge density Q (mC cm^{-2}) as a function of dipped layers for CeO_2 films at different sol concentrations: (*) 4.8×10^{-3} mol, (O) 7.2×10^{-3} mol, (×) 9.6×10^{-3} (at 500 °C).

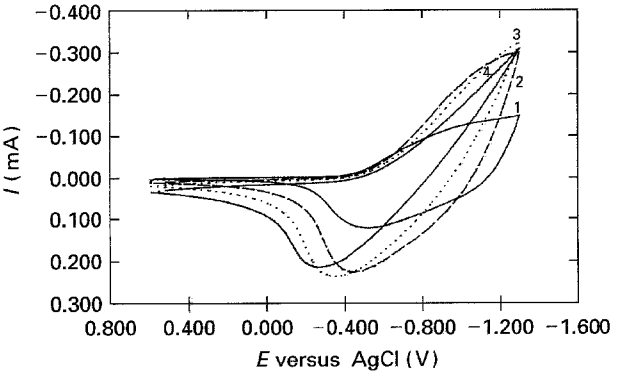

Figure 2 Cyclic voltammograms of CeO_2 films as a function of dipped layer thickness at constant sol concentration (7.2×10^{-3} mol) at a potential scan rate of 20 mVs^{-1} in 0.1 M LiOH. 1, one layer; 2, three layers; 3, five layers; 4, eight layers.

3. Results and discussion

3.1. Electrochemical investigation

Cyclic voltammetry (CV) was employed to investigate the usefulness of CeO_2 and CeO_2/SnO_2 dip-coated films as a counter electrode for a electrochromic device for "smart windows". This technique measures the capability of the films reversibly to intercalate and deintercalate mobile ions. In our work, all measurements were performed in 0.1 M LiOH.

The dependence of cyclic voltammogram (CV) on CeO_2 dip-coated films prepared from different sol concentrations was studied. The CV obtained revealed that the electrochemical response depended on the concentration used [14]. The peak current density of the films, prepared from the 7.2×10^{-3} mol and 9.6×10^{-3} mol in 20 ml (H_2O) starting sols, was very similar and much higher than for the film prepared from 4.8×10^{-3} mol in 20 ml H_2O. Chronocoulometric measurements were also performed for CeO_2 films prepared from the same concentration of sols with a different number of dipped layers. The charge capacity (mC cm^{-2}) refers to the amount of charge stored or extracted per cycle for an electrode and was recorded as a function of time (to 60 s) for each film. For three different concentrations (Fig. 1), it was found that charge density is closely connected with the concentration used and with the number of dippings. The charge density was higher if the starting concentration of used sol was high and the number of dippings was great.

According to the results obtained, the concentration of 7.2×10^{-3} mol was chosen for the preparation of pure CeO_2 and mixed CeO_2/SnO_2 dip coated films. In Figs 2 and 3 the CV measurement and chronocoulometric measurements are presented. It can be seen that when the number of dipped layer films is high, the CV response become greater and the amount of charge stored or extracted per cycle after 60 s is about 4 mC cm^{-2} for one layer and about 16 mC cm^{-2} for eight layers. As is shown in Table I, in the experimental part of our work, different CeO_2/SnO_2 dip-coated films were prepared. The concentration of SnO_2 added was maximally 50 mol%. For all of these, the cathodic and anodic total charge density, Q (mC), after 60 s was determined. In Fig. 3 the influence of added SnO_2 up to 17 mol% is presented. For that concentration, the amount of charge density, Q, was about 10 mC cm^{-2} for one layer and about 22 mC cm^{-2} for eight layers. The highest charge density for one layer was obtained after the addition of 17 mol% SnO_2. If the concentration was higher, the charge density began to decrease. So, for one layer the charge density after the addition of 25 mol% SnO_2 was about 7 mC cm^{-2}, for 33 mol% it was 6 mC cm^{-2}, and for 50 mol% it was 4.5 mC cm^{-2}.

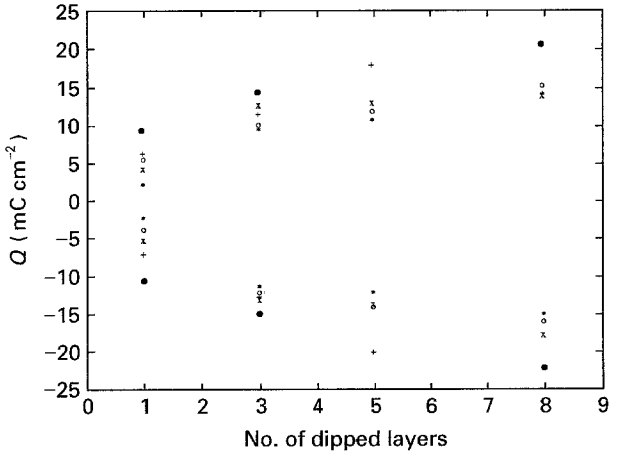

Figure 3 Cathodic and anodic total charge density Q (mC cm^{-2}) as a function of added SnO_2 and a number of dipped layers: (O) pure CeO_2; (*) 3.2 mol% SnO_2; (×) 6.25 mol% SnO_2; (+) 9.1 mol% SnO_2; (●) 17 mol% SnO_2.

The best sample with only one layer, prepared after addition of 17 mol% of SnO_2, was tested for voltammetric stability [14]. In each measurement the potential was swept for anodic (0.4) to cathodic potential (− 1.3) and then reversed to the initial value. The four hundred sweep mode was applied, and the CV for initial and last cycle (400th cycle) were compared. A slight diminishing in the CV after cycle 400 was observed, which we suppose to be related with changing, or more precisely, diminishing ability to intercalate and deintercalate Li^+ ions in the film. After

cycling, the film looks the same, without any visible changes.

Another phenomenon was found for samples prepared with the same mol% of added SnO_2, but with higher concentration of initial solution. For example, for the concentration of starting solution of cerium 4.8×10^{-4} with 9.1 mol% SnO_2 in 20 ml H_2O the charge stored or extracted was for one layer about 4 mC, and for three layers about 10 mC. Higher values were obtained if the starting solution was 7.2×10^{-4} mol with 9.1 mol% in 20 ml. Thus, for one layer, Q was equal to 7 mC cm^{-2}, and for three layers was equal to 12.5 mC cm^{-2}. This means that the preparations of counter electrodes with good ability for storing and extracting Li^+ ions is closely connected with concentrations used and with CeO_2/SnO_2 ratio. This is particularly evident if we compare the obtained CV response and Q values for one layer.

3.2. Structural characterization

Regarding the applied dispersion method for sol preparation, the influence of added NO_3^- ion for obtaining CeO_2 and CeO_2/SnO_2 thin films was followed with FT–IR spectroscopy. It is well known that different chemical species, such as proton or hydroxide, are important in the formation of the condensed phase from aqueous solutions. Different anions are usually added in order to control the shape and size of colloidal particles [15]. Sols prepared by the dispersion method are usually peptized with nitric acid. It has been found [1] that, when the nitric acid was added to dissolve a stoichiometric quantity of thoria, the rate of peptization depended upon the amount of acid added per 1 mol thoria for peptization.

According to Henry *et al.* [16], some anions, such as NO_3^-, are able to complex at a given hydrolysis ($h = 2$) with precursors only if they act as bidentate ligands. It has been confirmed by X-ray diffraction measurements on the basic salt of $ZrO(NO_3)_2.5H_2O$ that nitrates substitute two water molecules, thus giving rise to chain polymers $[Zr(OH)_2(OH)_2(NO_3)]_n^{n+}$ with terminal (NO_3^+) groups.

Absorbance spectra of freeze-dried samples are presented in Fig. 4 and were prepared as nujol mull (Table I). All spectra are characterized by the OH^- mode at 3400 cm^{-1} belonging to the hydrated species, and bands at 1630 cm^{-1} indicating the presence of water (typical bending). Bands at 1510, 1290 and 1035 cm^{-1} indicate the bidentate complex formations

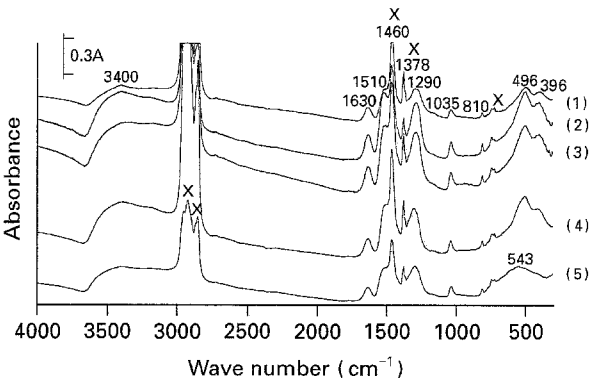

Figure 4 FT–IR absorbance spectra of xerogels at different concentrations of added SnO_2. 1, pure CeO_2 2, 6.25 mol% SnO_2; 3, 9.1 mol% SnO_2; 4, 17 mol% SnO_2; 5, 50 mol% SnO_2; (×) nujol bands.

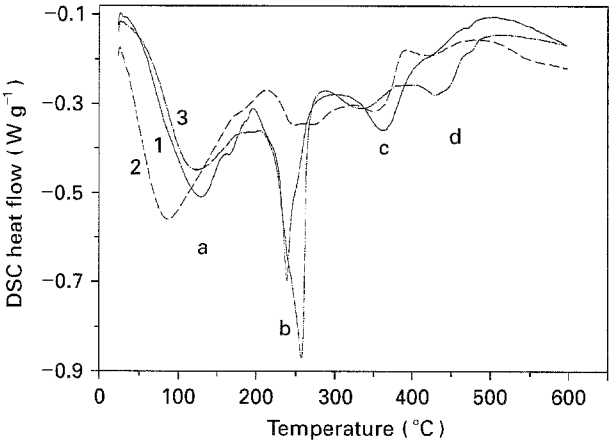

Figure 5 DSC for freeze-dried samples; 1, pure CeO_2; 2, 17 mol% SnO_2 in CeO_2; 3, 50 mol% SnO_2 in CeO_2. Endothermic transitions are labelled a, b, c and d.

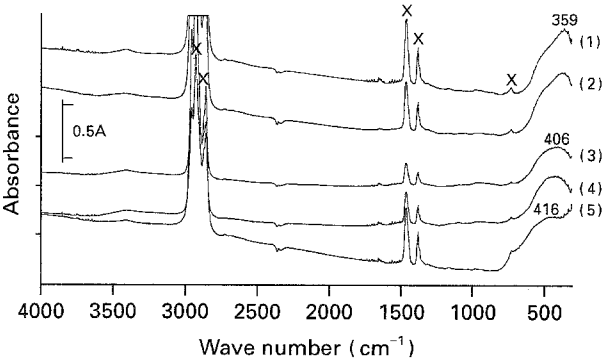

Figure 6 FT–IR absorbance spectra of samples heated at 500 °C at different concentrations of added SnO_2. 1, pure CeO_2; 2, 6.25 mol% SnO_2; 3, 9.1 mol% SnO_2; 4, 17 mol% SnO_2; 5, 50 mol% SnO_2; (×) nujol bands.

TABLE II Major temperature, T (°C), of endothermic DSC peaks and corresponding enthalpies ΔH (Jg^{-1}) for freeze-dried samples of pure CeO_2 powder and CeO_2/SnO_2 powders

Added SnO_2 (mol%)	a		b		c		d	
	T_{peak}	ΔH	T_{peak}	ΔH	T_{peak}	ΔH	T_{peak}	ΔH
0	114	51	233	23.6	358	27	436	4.5
3.2	114	81	242	57	356	28	–	–
6.25	118	147	256	34	349	22	436	8
9	95	169	244	39	354	22	421	4.6
17	86	193	250	22.1	364	15	427	4.4
50	115	73	258	88	335	14	444	10

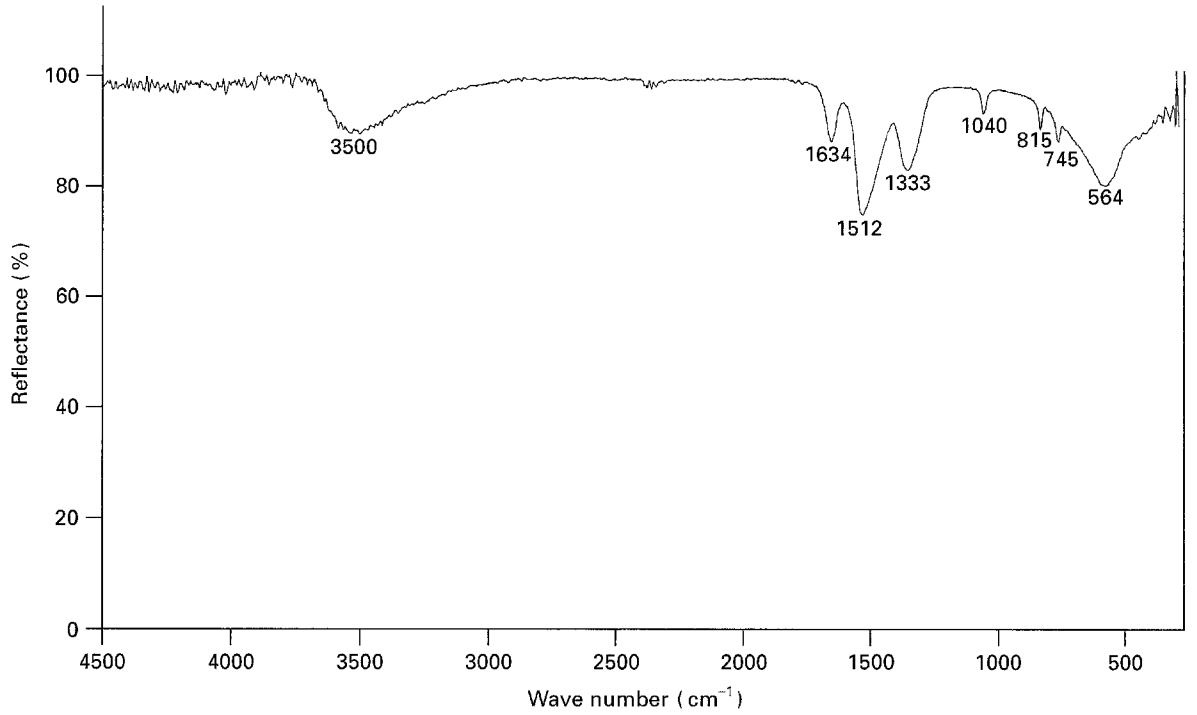

Figure 7 NGIA reflectivity spectra of pure CeO_2 (dried at room temperature).

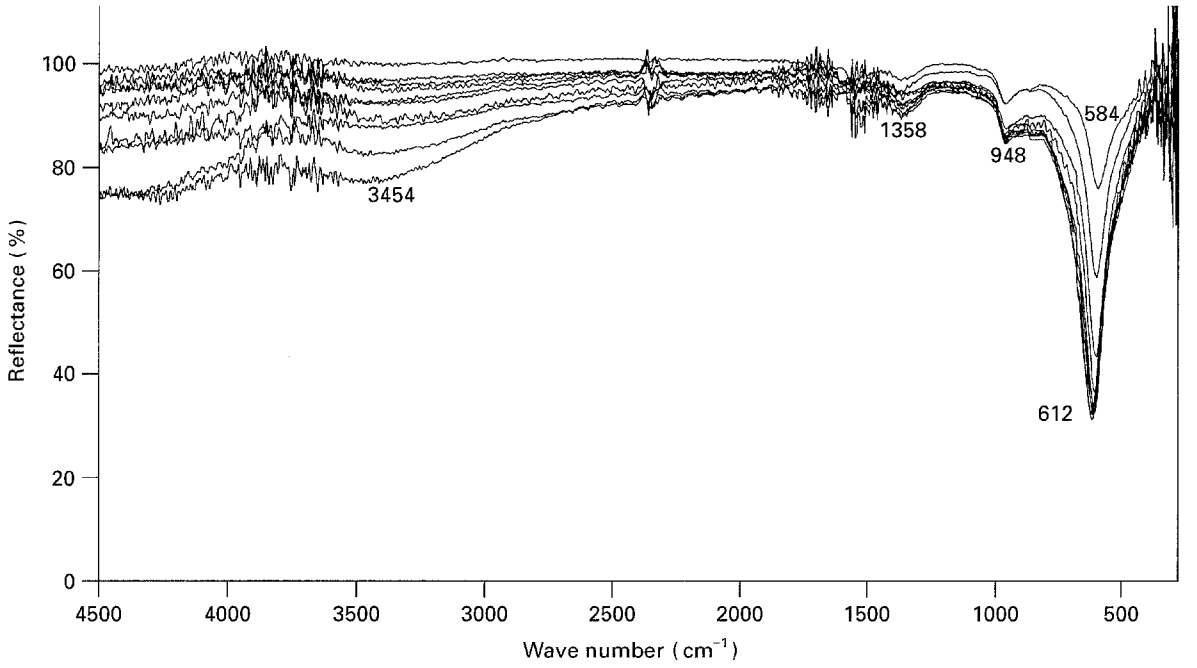

Figure 8 NGIA reflectivity spectra of pure CeO_2 (heated at 500 °C) for 1–10 dip-coated layers.

of NO_3^- groups according to the separation of the two highest frequency bands (220 cm^{-1}) [17, 18].

From Fig. 5 and Table II, four regions are evident (marked a, b, c and d) for DSC measurements. The first region (a) shows water release ($\approx$ 100 °C); the second (b) involves the expulsion of NO_3^- bidentate bonded groups which continue up to 500 °C (c, d). This finding is also corroborated by the inspection of corresponding IR spectra (samples heated at 500 °C) Fig. 6, from which no NO_3^- groups are observed to be present.

The reflectivity spectrum obtained by near grazing-incidence angle ($NGIA = 80°$) detected in the p-polarization on an aluminium substrate (one dip layer dried at room temperature) shows very similar spectra to those of freeze-dried samples. The characteristic bands for OH^- and NO_3^- groups are (Fig. 7) observed at approximately the same wavelength. Only very small shifts are observed. (10–100 cm^{-1}). The band at 564 cm^{-1} was observed for the same sample, which we attribute to Ce–OH mode. After heating the samples at 500 °C, all characteristic bands disappeared, except the band at 584 cm^{-1} (Fig. 8). The observed band appears at longitudinal optical frequencies, *LO* [2]. The p-polarized spectra have a peak near the frequency of the *LO* phonon of bulk CeO_2. The infrared absorption of bulk and thin-film CeO_2 were reported by Mochizuki [2], who studied his sample in the

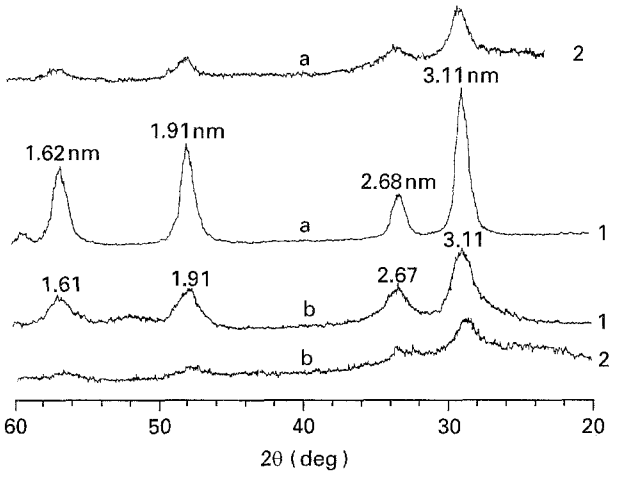

Figure 9 X-ray diffraction patterns of CeO_2 powder and thin dip-coating films heated at 500 °C: (a) pure CeO_2, (b) $CeO_2/SnO_2 = 1$.

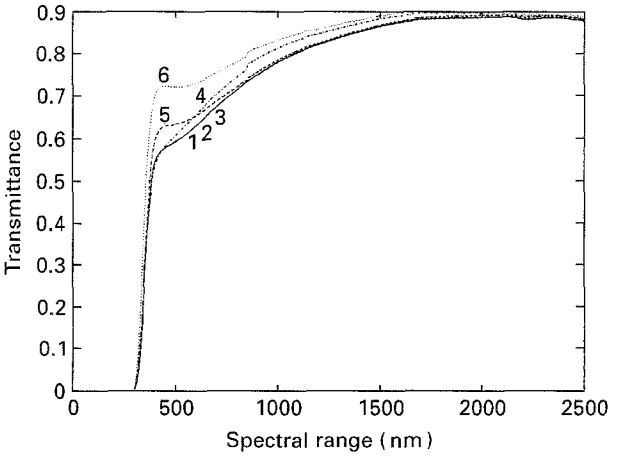

Figure 10 Transmittance (UV–VIS–NIR) spectra of CeO_2 with different concentrations of added SnO_2: 1, 3.2 mol% SnO_2; 2, 6.25 mol% SnO_2; 3, 9.1 mol% SnO_2; 4, 25 mol% SnO_2; 5, 33 mol% SnO_2; 6, 50 mol% SnO_2.

region 200–1000 cm^{-1}. He found that the shape of the reflectivity spectrum in the spectral region 400–600 cm^{-1} was slightly specimen dependent. Reflectivity spectra were analysed by means of the oscillator dispersion model. The main ν_1 resonance frequency at 272 cm^{-1} was identified with T_{1u} transverse optical phonon frequency, ν_{TO}, near zero wave vector, and the T_{1u} transverse optical phonon frequency, ν_{LO}, was 585 cm^{-1} near zero wave vector.

In Fig. 8, reflectivity at *NGIA* is determined for dip-coated samples on aluminium treated at 500 °C, with various thicknesses. The reflectivity was determined by measuring the intensity, reflected by the substrate without CeO_2 film at the same incidence angle. The band at 584 cm^{-1} is shifted after ten layers at 620 cm^{-1}.

X-ray diffraction measurement of powders and thin films, heated at 500 °C, showed formations of crystalline cerianite (Fig. 9). According to X-ray measurments, the addition of SnO_2 did not influence the position of peaks at $2\theta = 28.6°$, 33.34°, 47.5°, and 56.5° and only increased broadening of diffraction lines when an increased amount of SnO_2 was observed.

NGIA spectra for dip-coated samples on aluminium, treated at 500 °C with 17% SnO_2 reveal approximately the same spectra and dependence upon the multilayer dip-coating.

4. Optical properties of coatings

The transmission spectra of CeO_2 and $CeO_2/SnO_2 > 1$ for one dip layer, on ITO cover glass previously treated at 500 °C as a function of added SnO_2, are presented in Fig. 10. The transmission cut-off in the spectral range at 300–400 nm is observed. The addition of SnO_2 improved the transmission, and is highest ($T_s = 0.778$) after addition of 50 mol% SnO_2. Spectra obtained for pure CeO_2 thin films and after the addition of 17 mol% SnO_2 were very similar. The calculated solar transmittance, T_s (Table III) for all samples in the spectral range 0.3–2 μm were high ($T_s > 64\%$) and T_s for approximately the same thicknesses of applied pure CeO_2 and CeO_2 with 17 mol% SnO_2, are 20% lower than calculated T_s of pure ITO on the glass.

TABLE III Solar transmittance, T_s, of pure CeO_2 and CeO_2 with different concentrations (mol%) of added SnO_2 (1–6) on ITO covered glass

Sample	SnO_2 (mol%)	T_s 0.3–2.0 μm
	0	0.645
1	3.2	0.645
2	6.25	0.645
3	9.10	0.645
	17.0	0.648
4	25	0.712
5	33	0.715
6	50	0.775
ITO		0.80

5. Conclusion

The aqeuous-based process was successfully used for the preparation of CeO_2 and CeO_2/SnO_2 dip-coating films for a counter electrode. The best samples obtained at 17 mol% SnO_2 have a very good possibility for the intercalation/deintercalation of Li^+ ions. The cathodic and anodic charge densities of 10 and 22 mC were obtained for one and eight layers, respectively.

Acknowledgement

This work was supported by the The Ministry of Science and Technology, Republic of Slovenia, research contract P1-5012-104-93.

References

1. C. W. TURNER, *Ceram. Bull.* **70** (1991) 1487.
2. S. MOCHIZUKI, *Phys. Status. Solidi* **114** (1982) 189.
3. K. EGUCHI, T. SETOGUCHI, T. INONE and H. ARAI, *Solid State Ionics* **52** (1992) 165.

4. C. A. HAMPEL, *Glass Ind.* **41** (1960) 82.
5. P. BAUDRY, A. RODRIGUES, M. AEGERTER and L. O. BULHÕES, *J. Non-Cryst. Solids* **121** (1990) 319.
6. R. D. RAUH and S. F. COGAN, *Solid State Ionics* **28–30** (1988) 1707.
7. U. LAVRENČIČ ŠTANGAR, B. OREL, I. GRABEC, B. OGOREVC and K. KALCHER, *Solar Energy Mater. Solar Cells* **31** (1993) 171.
8. Z. CRNJAK OREL, M. G. HUTCHINS and G. McMEEKING, *ibid.* **30** (1993) 327.
9. W. F. CHU, R. HARTMANN, V. LEONHARD and G. GANSON, *Mater. Sci. Eng.* **B13** (1992) 235.
10. Z. CRNJAK OREL, B. OREL, M. HODOŠČEK and V. KAVČIČ, *J. Mater. Sci* **27** (1992) 313.
11. Z. CRNJAK OREL, B. OREL and M. KLANJŠEK GUNDE, *Solar Energy Mater.* **26** (1992) 105.
12. A. ATKINSON and R. M. GUPPY, *J. Mater. Sci.* **26** (1991) 3869.
13. R. L. NELSON, J. D. F. RAMSAY and J. L. WOODHEAD, *Thin Solid Films* **81** (1981) 329.
14. Z. CRNJAK OREL and B. OREL, in "Optical Materials Technology for Energy Efficiency and Solar Energy Conversion" XIII, 2255 (1994) 285, edited by V. W. Hwer, C. G. Granqvist and C. M. Lampert.
15. W. P. HSU, L. RONNQUIST and E. MATIJEVIĆ, Langmuir **4** (1988) 31.
16. M. HENRY, J. P. JOLIVET and J. LIVAGE, in "Chemistry, Spectroscopy and Applications of Sol-Gel Glasses", edited by R. Reisfeld and C. J. Jørgensen. (Springer, Berlin, Heidelberg, 1992) pp. 153–207.
17. A. A. DAVYDOV, "Infrared Spectroscopy of Adsorbed Species on the Surface of Transition Metal Oxides" (Wiley, Chichester, 1990).
18. K. NAKAMOTO "Infrared and Roman Spectra of Inorganic and Coordination Compounds", (Wiley, New York, 1978).

Received 8 April
and accepted 25 November 1994